

# HIGH LEVEL SOFTWARE FOR BEAM 6D PHASE SPACE CHARACTERIZATION

V. Martinelli\*, D. Alesini, M. Ferrario, A. Giribono, S. Pioli, C. Vaccarezza, A. Variola,  
INFN-LNF - Frascati National Laboratory, Rome, Italy  
A. Bacci, INFN-Milano - Section of Milano, Italy

## Abstract

Operation of modern particle accelerators require high quality beams and consequently sensitive diagnostic system in order to monitor and characterize the beam during the acceleration and transport. A turn-key high level software BOLINA (Beam Orbit for Linear Accelerators) has been developed to fully characterise the 6D beam phase space in order to help operator during commissioning with an easily scalable suite for any high brightness LINAC. In this work will be presented the diagnostic toolkit as designed for the ELI-NP Gamma Beam System (GBS), a radiation source based on the Compton back scattering effect able to provide tunable gamma rays, in the 0.2-20 MeV range, with narrow bandwidth (0.3%) and a high spectral density ( $10^4$  photons/sec/eV). BOLINA suite is designed to be machine independent, thanks to the file exchanges with the EPICS based control system. Simulation of raw data of the ELI-NP GBS accelerator has been used to test the capabilities of the diagnostic toolkit.

## INTRODUCTION

The BOLINA suite starts from the generic operator needs during commissioning of a machine like the new Gamma Beam System (GBS) of the ELI-NP project [1]. All the BOLINA's routines are written in Python, permitting to design an object oriented suite with dedicated independent modules for each measurement. The raw data and the machine parameters (i.e. magnet excitation curves, element positions, etc ...) are read from an external file. In this way the software is machine independent and it can run both on-line and off-line. When a measurement is required, BOLINA sends the proper command/request to EPICS control system [2] which calls the involved accelerator devices and produces a file containing the data readout of raw experimental data. BOLINA takes such raw data, elaborate the measurements and send back these results to the control system in order to log them as sketched in Fig. 1. In this paper is presented the diagnostic toolkit, part of the BOLINA high level software, that gather all the measurements and the measurements-errors. On this purpose raw data for BOLINA have been simulated through multiple tracking runs of ELI-NP-GBS accelerator. Such kind of simulations have been performed, for the injector, with ASTRA [3] tracking code, since it takes into account the space charge forces, while booster and transfer lines tolerances have been studied with elegant [4 - 7].

\* valentina.martinelli@lnf.infn.it

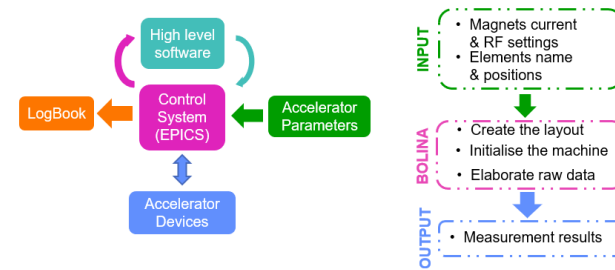


Figure 1: On the right the interaction of BOLINA with the control system; on the left the modular structure that permit the machine independency.

## THE DIAGNOSTIC TOOLKIT

The diagnostic stations along the machine are equipped with YAG and OTR screens and used to acquire the image of the transverse spot size. BOLINA provides all the other beam parameters such as the transverse emittance, energy and the energy spread, and with the help of a RF deflector the bunch length and the longitudinal phase space.

Here we report as an example the simulation of measurements on the first diagnostic station after the RF gun. Thanks to the modularity of code, implemented through file exchanged with the control system that share all the machine parameter such as the monitor positions and magnetic characteristics (magnetic length, magnetic field, and dipoles excitation curves) it is true for any diagnostic stations in the whole LINAC.

### Energy Measurement at the Gun Exit

The beam transverse spot size and the centroid position can be measured by means of YAG screens. The centroid position move horizontally (or vertically) changing the horizontal (or vertical) field of an upstream steerer. To simulate raw data at the gun exit and studying the sensitivity of the beam measurement we use the ASTRA tracking software. The RF gun field, as the emittance compensation solenoid, is imported from a bi-dimensional map while the steering magnet has been implemented as a rectangular dipole magnet with uniform magnetic field  $B_0$ . Its length is equal to the effective magnetic length  $L_{eff}$ , that takes into account the profile of the magnetic field  $B_y(z)$  included longitudinal fringe fields. Naming the drift space length  $L_{drift}$  as the distance between the steerer and the first YAG screen downstream the gun, the beam centroid position can be evaluated from easy geometrical consideration  $C_x = L_{drift} \tan(\theta)$ , where  $\theta$  is the beam deflection defined as:  $\theta = \frac{L_{eff}}{R}$ . In our

case the small angle approximation is valid and beam energy at the gun exit can be estimated by plotting and fitting the beam centroid position (see Fig. 2) as function of the magnetic field; through the linear fit coefficient,  $m$ , it is possible to find the beam energy after the RF gun.

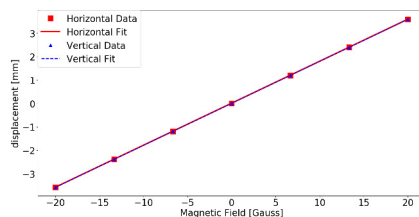


Figure 2: Energy at the gun exit simulation. Marker represent simulated raw data, while line is the fitted curve.

$$p = \frac{L_{drift}[m]c[m/s]L_{eff}[m]}{m[mm/Gauss]} 10^{-3} \quad (1)$$

By calling the momentum of the beam at the gun exit given by Astra simulations,  $p_{real}$ , and the measured momentum obtained by the fit using the formula 1 is called  $p_{meas}$  we defined the relative error as  $\Delta P/P = \frac{p_{real}-p_{meas}}{p_{real}}$  that is equal to 0.009% as expected, on both steerers.

### Energy and Energy Spread Measurement

Dipole magnets deflect a beam particles depending on their energy so introducing dispersion. The beam profile after the dipole will therefore allow determine the energy profile and consequently the average energy and rms energy spread. The measurement has been tested using elegant simulation. The only difference from the formula used for the beam energy at the gun exit is that the the drift space is the distance from the arc centre to the target position:  $L_{drift} = D + \frac{R}{2} \sin(\theta)$ . The result obtained by the diagnostic tool,  $E_{meas}$ , has been compared with the "real" data given by elegant simulation,  $E_{real}$ , with acceptable relative error  $\frac{\Delta E}{E} = (E_{real} - E_{meas})/E_{real} = 0.005\%$ .

Using a bending magnet it is possible to measure the energy spread of the beam,  $\frac{\Delta p}{p} = \delta$ . The beam size depends on the dispersion function  $D(s)$ . The beam size measured ,reported in Fig. 3 at a given position depend on the energy spread, the dispersion function and the monochromatic contribute to the beam size  $\sigma_\beta^2$ , as in formula 2.

$$\sigma_x = \sqrt{\sigma_\beta^2 + D^2 \sigma_{\frac{\Delta p}{p}}^2} \quad (2)$$

For this reason optimum resolution is achieved using quadrupole to focus the beam in the horizontal plane and measuring the beam energy spread where the monochromatic contribute to the beam size is small and the beam dispersion is large. By using the same simulations used for the beam energy measurement, focusing first the beam

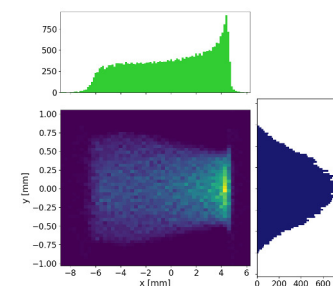


Figure 3: Simulated spot on the screen downstream the dipole.

especially in the horizontal axis and then measuring the simulated spot size the energy spread is given by formula:

$$\frac{\sigma_p}{p} \approx \frac{\sigma_x}{D} = \frac{\sigma_x}{R(1 - \cos(\frac{L_{eff}}{R})) + \sin(\frac{L_{eff}}{R})L_D} \quad (3)$$

The simulated measurement is totally in accord with the aspected value given by the simulation, indeed the relative error defined as  $\frac{\Delta \delta}{\delta} = (\delta_{real} - \delta_{meas})/\delta_{real} = -0.367$  is below the 0.4%.

### Beam Length and Longitudinal Phase Space Measurement

The Radio Frequency Deflector (RFD) provides a transverse kick to the incoming electron bunch. Since the RF kick depends on the longitudinal position of the bunch particles a correlation is induced between the bunch longitudinal dimension and the bunch vertical dimension at a screen, placed after the RFD. Therefore, the electron bunch length can be obtained through vertical spot size measurements after a proper calibration. Using a dispersive element together with the RFD permits to have projected on a YAG or OTR screen the Longitudinal Phase Space (LPS). Since the beam has a finite transverse emittance, at the zero crossing, the distribution of the deflected bunch at the screen position is a superposition of the transfer beam size  $\sigma_{y,off}$  and the longitudinal beam profile  $\sigma_t$ :

$$\sigma_y = \sqrt{\sigma_{y,off}^2 + \sigma_t^2 K_{cal}^2} \quad (4)$$

where  $K_{cal} = (V_0/E)\omega_{RF}L_{drift}$  has been defined as the calibration factor at the zero crossing. This coefficient depend on the characteristic of the RFD: the transverse integrated kick along the structure  $V_0$ , the RFD phase  $\phi$  and frequency  $\omega_{RF}$ , the beam energy  $E_0$  and on the lattice downstream the RFD, in our case a drift of length  $L_{drift}$ . In equation 4 is shown that the transverse distribution is a sum in quadrature of the transverse beam dimension  $\sigma_{y,off}$  when the RFD is turned off, plus the weighted beam length,  $\sigma_z$ , where the weight is the calibration factor. Therefore to measure the beam length with the standard technique the spot on the screen, must be focus with quadrupoles, in order to have a small contribute of  $\sigma_{y,off}$  respect to  $K_{cal}\sigma_t$ .

The measurements can be self calibrated through the vertical bunch centroid  $C_y(\phi)$  varying the deflecting voltage phase in a small range near the zero crossing [8], as reported in Fig. 4. At least a more accurate measurement of the beam

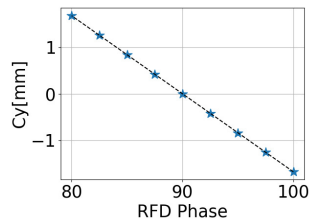


Figure 4: Simulated calibration factor measurement. Marker represent simulated raw data, while line is the fitted curve.

length can be done by taking into account the correlation between vertical and longitudinal planes. An accurate description of all contributes can be found in literature [9]. This technique is based on the measurements of the vertical spot size at screen after the RFD for both zero crossing phases. The raw data analysed from the diagnostic toolkit are simulated with `elegant`. The RFD has an integrated deflecting Voltage of 1 MV and the screen used for the measurement is on the straight part of the LINAC. From simulated measurement result that the beam length relative error is  $\Delta\sigma_t/\sigma_t = (\sigma_{t,real} - \sigma_{t,meas})(\sigma_{t,real}) = -0.35\%$  that is a satisfactory result. The same procedure has been done for the other zero crossing phase, with the RFD phase at - 90 degree. In this simulation the beam has the same spot size of the result at 90 deg while the calibration term is equal in module but has opposite sign as aspected.

By using both a dispersive element and the radio frequency deflector is possible to have an online representation of the longitudinal phase space on a YAG or OTR screen. Projecting the beam on the screen where the dispersion function is big, for example after a dipole, is possible to measure the energy distribution of the beam for measuring the beam energy spread. If the beam is simultaneously deflected by using a RF deflector it is possible to project at the same time the beam energy distribution and longitudinal beam projection. Here is reported the beam longitudinal phase space obtained with `elegant` simulation using the same dipole and the RFD used for the previous measurement of energy, energy spread and beam length.

In Fig. 5 is reported the simulated trace space at the screen position, on the right the measured spot measured on the screen representing the LPS measurement, where the x axis correspond to the beam energy while on the y axis the longitudinal coordinate of the particles. Comparing the measured spot size when RFD is turned off, with the LPS of the simulation, at the same screen position no significant differences can be notice.

### Beam Emittance Measurement

The emittance like the bunch length, is one of the most important parameters for high brightness beam. The method

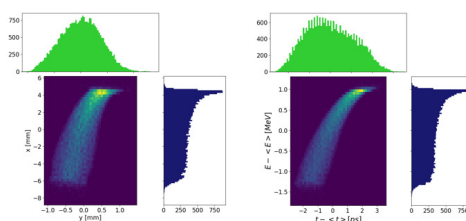


Figure 5: On the left the simulated trace spaces at the screen position, on the right the measured spot on the same screen.

used for ELI-NP-GBS emittance measurement, geometrical  $\epsilon$  and normalised  $\epsilon_n = \epsilon\beta\gamma$  ( $\beta$  and  $\gamma$  are the Lorentz factors), is the quadrupole scan technique. The theory of this method is well known, usually is developed assuming a mono energetic beam described by the symmetric Beam Matrix,  $\Sigma$ , as function of Twiss parameters  $(\alpha, \beta, \gamma, \Sigma)$ . The geometric emittance is than defined as  $\epsilon = \sqrt{\det(\Sigma)} = \sqrt{< x^2 > < x'^2 > - < xx' >^2}$ . The square of the beam size  $\Sigma_{11}$  ( $\sigma_y^2$ ) at a generic point  $P_i$  from a point  $P_0$  is function of the Transfer Matrix terms  $R_{ij}$ . In the case used in ELI-NP-GBS for the beam emittance measurement the Transfer Matrix is given by the product of the drift matrix with the quadrupole matrix with geometric strength  $k$ . Assuming that the length of the quadrupole,  $l_q$ , is small as respect to the drift length,  $L_{drift}$ , we can use the thin lens approximation, and the square of the beam size can be expressed as a parabolic function in  $k$  that can be find using a parabolic fit function:  $\sigma_y^2 = (L_{drift}^2 l_q^2 \Sigma_{0,11})k^2 + 2(L_{drift} l_q \Sigma_{0,11} + L_{drift}^2 l_q \Sigma_{0,12})k + (\Sigma_{0,11} + 2L_{drift} \Sigma_{0,12} + L_{drift}^2 \Sigma_{0,22})$ . In order to have a defined spot and avoiding non-linearities of the quadrupole, the scan of quadrupole strength must be done near the beam waist. Moreover the parabolic function fit near the vertex is more sensitive to the coefficient variation.

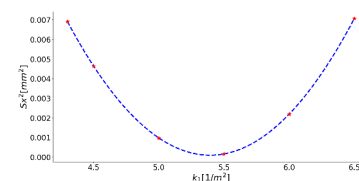


Figure 6: Horizontal emittance measurement simulation. Marker represent simulated raw data, while line is the fitted curve.

The emittance measurement has been simulated using `elegant` tracking code, simulated measurement data are report in Fig. 6. This type of quadrupole focus both in the horizontal x axis, given a positive magnetic strength, and in the vertical y axis using a negative strength by changing the current sign. The beam vertical normalised emittance from the simulation is the same of horizontal one. The `elegant` simulation emittance  $\epsilon_{ny,real}$  has an relative error of 0.24% from the estimated value,  $\epsilon_{ny,meas}$  that confirm the goodness of the simulation toolkit and the used method.

## REFERENCES

- [1] O. Adriani *et al.*, “Technical design report eurogammas proposal for the eli-np gamma beam system.” in *arXiv:1407.3669 [physics.acc-ph]*.
- [2] S. Pioli *et al.*, “The Turn-key Control System for the ELI-NP Gamma Beam System”, in *Proc. 7th Int. Particle Accelerator Conf. (IPAC'16)*, Busan, Korea, May 2016, pp. 4091–4093. doi:10.18429/JACoW-IPAC2016-THPOY003
- [3] *A Space Charge Tracking Algorithm: ASTRA* <http://www.desy.de/~mpyflo/>
- [4] *Elegant software* <https://www.aps.anl.gov/Accelerator-Operations-Physics/Software#12345>
- [5] A. Bacci *et al.*, “Electron Linac design to drive bright Compton back-scattering gamma-ray sources.”, in *Journal of Applied Physics* 113.19 (2013): 194508
- [6] C. Vaccarezza *et al.*, “Optimizing rf linacs as drivers for inverse compton sources: the eli-np cases”, in *Proc. 27th Linear Accelerator Conf. (LINAC2014)*, Geneva, Switzerland, August 31-September 5, 2014, MOIOB02. <http://jacow.org/LINAC2014/papers/moiob02.pdf>
- [7] A. Giribono *et al.*, “6D phase space electron beam analysis and machine sensitivity studies for ELI-NP GBS”, in *Nuclear Instruments and Methods in Physics Research Section A: Accelerators, Spectrometers, Detectors and Associated Equipment* vol. 829 (2016) pp. 274–277.
- [8] D. Alesini *et al.*, “Sliced beam parameter measurements”, in *Proc. of DiPAC-2009*, Basel, Switzerland, 2009, pp.146-150.
- [9] L. Sabato *et al.*, “RF deflector based measurements of the correlations between vertical and longitudinal planes at ELI-NP-GBS electron LINAC.” in *Proc. of Int. Beam Instrumentation Conf.*, Grand Rapids, Michigan, USA, 20–4 August, 2017.